

**When the statistics of image reconstruction are considered, the anisotropies in the cosmic microwave background reported by COBE appear to be less than the systematic errors**

**Keith S Cover  
Keith@kscover.ca**

**Abstract**

In the official analysis, sky maps reconstructed from the data measured by the Cosmic Background Explorer's (COBE) differential microwave radiometer (DMR) showed structure in the cosmic microwave background (CMB) at 10 ppm. However, the statistical methods used in the official analysis were intended for the detection of signal in measurements provided by direct detection, such as those that will be measured by the Planck satellite. In this paper, the COBE 4 year data set was reanalysed by extending the statistical concept of rejecting the null hypothesis to image reconstruction. The primary null hypothesis to be rejected is that there are no anisotropies outside of the galactic band. In contrast to the official COBE analysis, which found systematic errors were no more than approximately 1 part in 5 of the reported anisotropies in the sky maps, the reanalysis indicates that the systematic errors are closer to three times the reported anisotropies. The source of the additional systemic error in the reanalysis is the non ideal behaviour of the instrumentation noise due to calibration drift compounded by image reconstruction. The possibility of non ideal noise was only partially considered in the official analysis. The results of the reanalysis raise questions about the reliability of the COBE detection of the anisotropies at 10ppm. The high correlation between the COBE sky maps and other reported detections of the anisotropies might be explained by the use of common information in the data analysis. The single beam antenna and low noise receivers of the soon-to-be-launched Planck satellite should permit direct measurement of the 10ppm anisotropies and provide definitive evidence as to their existence or non existence.

## INTRODUCTION

Precise and accurate measurement of anisotropies in the cosmic microwave background (CMB) would provide a treasure trove of information on the cosmos. As a consequence, tremendous effort has been expended on trying to detect and measure any anisotropies. These efforts have included two satellite missions that have published results, the Cosmic Background Explorer (COBE) (Smoot et al. 1992; Bennett et al. 1996) and the Wilkinson Microwave Anisotropy Probe (WMAP) (Bennett et al. 2003; Spergel et al. 2003). In addition, the Planck satellite is scheduled to be launched in early 2008 (Tauber 2004).

The official COBE analysis reported detecting anisotropies at roughly 10 ppm of the CMB temperature. The WMAP mission closely followed the COBE acquisition and reconstruction strategy but improved on the spatial resolution and reported detecting similar anisotropies. Both COBE and WMAP used a differential microwave radiometer (DMR). The DMR's, rather than directly measuring the intensity of the CMB at each point in the sky, measured the difference between two widely separated beams. For COBE the separation was  $60^\circ$ . For each satellite, a sky map of the fluctuations in the intensity of the CMB at each point in the sky was then reconstructed by finding the sky map that was most consistent with the DMR measurements in the maximum likelihood sense.

A major impediment to measuring the anisotropies in the CMB is the dust concentrated near the galactic plane. As the dust at the galactic centre is up to 1000 times brighter than the reported anisotropies in the CMB (Barnes et al. 2003), great care has been taken to ensure the dust signal does not contaminate the measurements away from the galactic band, including during the image reconstruction. While most of the dust lies within  $20^\circ$  of the galactic plane, at some longitudes it extends several degrees further (Kogut et al. 1996).

An inherent problem in designing any reconstruction algorithm is dealing with the nonuniqueness of the result – the fact that many different sky maps can be consistent with the same data set (Press et al. 1992). The official COBE analysis dealt with the nonuniqueness by using the sky map with the maximum likelihood fit to the data. Therefore, of all the sky maps that fit the data, the sky map that fit data with the smallest  $\chi^2$  measure (Press et al. 1992) was used. Thus, the official analysis overlooked the variety of other sky maps that were also consistent with the same data set, within a reasonable confidence limit of  $\chi^2$ , and the additional uncertainty this adds to reliable detection of the anisotropies.

By all accounts the COBE team put tremendous time, care and effort into ensuring the reported detection was as reliable as possible (Kogut et al. 1992; Smoot 1993; Mather & Boslough 1996). However, the author can find nothing in the literature to suggest that anyone applied statistical tests for the existence of the anisotropies that were designed for reconstructed images. While it is a common practice when interpreting reconstructed images to not explicitly take the reconstructed nature of the images into account, and instead use statistical measures intended for direct measurements, it leaves the analysis incomplete and prone to confusing and misleading results.

The maximum likelihood criterion has been widely used to design image reconstruction algorithms for many years. While it has important successes it has also performed less well than expected on some problems. For example, in designing multiexponential reconstruction algorithms, its results are often disappointing (Istratov and Vyvenko, 1999). Also, while maximum likelihood is a popular way to derive the discrete Fourier transform reconstruction algorithm, as is well known, the resulting reconstruction algorithm generates sidelobes (also called Gibb's phenomena or truncation artefacts) when applied to signals with large peaks. These sidelobes if not taken into account by interpreters can lead to false positive detection of signal: for example magnetic resonance image (MRI) reconstruction (Wood and Henkelman 1985; Frank et al. 1997).

Another possible source of false positive signals that can be compounded by image reconstruction is non ideal noise. Ideal noise has tidy statistical properties including the well known rule that the standard deviation of the noise reduces by the square root of the number of averages. COBE used averaging extensively to improve the signal to noise (SNR) of the data before image reconstruction. Also, the linear nature of the maximum likelihood image reconstruction algorithm is particularly sensitive to non ideal noise. In addition, estimation of the error in the official analysis of the COBE used simulations that assumed ideal noise. The 0.7% uncertainty in the calibration of the COBE data over the 4 year mission may cause a significant violation of the ideal noise assumption as the noise probability distribution is affected by the error in the calibration.

Selection of the best statistical test for the detection of a signal in a reconstructed image is an unresolved issue in many fields. For example, the multiexponential reconstruction problem is much simpler to state mathematically than COBE's but is also nonunique. There is no consensus on how to reconstruct multiexponential decays. A particular problem in multiexponential reconstruction, the myelin water peak detection problem, is surprisingly similar to the CMB anisotropy problem. Both techniques are trying to detect a small signal which is adjacent to a much larger one and both problems are approached using reconstruction algorithms. Indeed, the idea of generalising the concept rejecting the null hypothesis to image reconstruction and the modified maximum likelihood algorithm used in this paper were originally designed by the author for the multiexponential reconstruction problem of in vivo myelin water detection (Cover 2006).

For the COBE reconstruction problem, to test the null hypothesis that the anisotropies outside the galactic band were zero, a reanalysis was completed using a modified maximum likelihood reconstruction algorithm that forced all pixels to zero that were beyond a specified number of degrees from the galactic equator. The specified number of degrees was then varied from  $90^\circ$  to  $0^\circ$  and the best fit by the  $\chi^2$  measure was calculated for each. The sky maps and  $\chi^2$  values were then examined to determine if the null hypothesis could be rejected with any significant probability. As a double check on the analysis, a second null hypothesis, that each of the sky maps contained no signal, was also tested.

This paper is not the first to raise questions about the results reported by COBE and WMAP. Concerns about the unusual characteristics of some of the results have been

raised previously (Starkman and Schwarz 2005). Nevertheless, it is essential for the progress of science that the fundamental basis for assessing the reliability of any experimental results be the quality of the experimental technique and analysis rather than the consistency of the results with various theories.

## THEORY

When trying to detect a signal with direct measurement - such as by the soon-to-be-launched Planck satellite - the question is whether the measured value is sufficiently different from zero. The statistical test used is generally presented as a "null hypothesis" that must be rejected to a sufficient confidence level. In the Planck direct measurement case, the null hypothesis is that the measured value is zero. Assuming the measured value has ideal noise, the confidence level is often specified in terms of the number of standard deviations of the noise, with higher values indicating more confidence (Press et al., 1992). As each location on the sky will be measured independently of all other measured by the Planck satellite, each measured value can be tested independently from all other measures - assuming correct calibrations have been applied.

With COBE's differential measurement, no location in a sky map is measured independently of any others, thus no location should be tested for nonzero value independent of all others. Thus, for COBE, a reliable statistical test should be valid at the level of the sky map rather than individual pixels. Therefore, it is proposed that, the null hypothesis should be extended to image reconstruction by formulating it in terms of sky maps instead of the values of individual pixels (Cover 2006). For COBE the null hypothesis we are interested in rejecting is that there are no anisotropies outside the galactic band.

Underpinning most theories of image reconstruction is the familiar but important concepts of ideal signal and ideal noise. Ideal signal is assumed to maintain exactly the same value over all measurements. Ideal noise is usually assumed to be Gaussian, uncorrelated and maintain exactly the same distribution over all measurements (stationarity). Ideal noise is also assumed to be added to the ideal signal (additivity). A widely known and very useful property of ideal noise is that it obeys the square-root-of-N rule under averaging, where N is the number of data points. Thus, for ideal noise, the SNR ratio of data can be improved by a factor of 1000 by averaging together 1,000,000 measurements of the same signal. In the official analysis of the COBE data, the temperature variations of the anisotropies from the CMB are assumed to be ideal signal and the instrumentation noise, after calibration, is assumed to be ideal noise.

A widely used measure of the consistency of a model with a data set is the  $\chi^2$  value. In the COBE 4 year analysis the models are the possible sky maps and the data are the differential measurements over the 4 years. Because of the nature of the COBE measurements, the differential measurements are often referred to as the time ordered data (TOD). The equation for calculating the  $\chi^2$  value is

$$\chi^2 = \sum_{\tau} \left[ \frac{D_{ij}(t) - (T_i - T_j)}{\delta_{ij}(t)} \right]^2 \quad (1)$$

over the time,  $t$ , where  $D_{ij}(t)$  is the TOD,  $\sigma_{ij}(t)$  is the noise of the pixel pair,  $ij$ , observed at time  $t$  (Kogut et al. 1996). The larger the value of  $\chi^2$  the poorer the fit of the data to a potential sky map,  $T_i$ . Assuming ideal signal and noise, a large value for  $N$ , and that the sky map,  $T_i$ , is the true (but unknown) sky map, the expected value for  $\chi^2$  is  $N$ , and the standard deviation of  $\chi^2$  is  $(2N)^{1/2}$  (Press et al. 1992). Thus, for any proposed sky map we can calculate a confidence limit that the sky map is consistent with the data. The confidence limit is usually given in terms of the number of standard deviations the  $\chi^2$  value of the proposed sky map falls within the expected mean of the  $\chi^2$  value although, if desired, it can be converted to a p-value.

If we could show that all of the sky maps within a specified confidence level of the expected mean of the  $\chi^2$  value had anisotropies, then the null hypothesis would be rejected to the specified confidence level. Assuming the confidence level was sufficiently high, the anisotropies would be definitively detected. However the question arises, if we found a single sky map consistent with the data to within the confidence limit that had no anisotropies, would the null hypothesis still be rejected?

It is possible to calculate a probability density of a particular sky map directly from the  $\chi^2$  using the equation

$$\text{Prob}(\chi^2) = k \exp\left(-\frac{1}{2}\chi^2\right) \quad (2)$$

(Press et al. 1992 p 820) where  $k$  is a constant independent of  $\chi^2$ . Thus the probability density of any sky map is completely and uniquely determined by its  $\chi^2$  measure of fit to the data. A consequential property of the relationship between  $\chi^2$  and the probability density is that the probability density strictly decreases with increasing  $\chi^2$ . It is important to note that, although there is sufficient information to assign a probability distribution to the  $\chi^2$  value, the TOD does not have sufficient information to assign probabilities to individual sky maps, only probability densities can be assigned. The probability of a model, however, cannot be calculated without prior information (Tarantola 1987). As no reliable prior information exists for the COBE sky maps reliable probabilities cannot be calculated for individual sky maps.

Therefore, if there is at least one sky map, that is consistent with the data with a specified confidence level that does not have anisotropies, it is impossible to assign a probability to the existence of the anisotropies based only on the information in the data alone. Thus, all that can be said is that within the specified confidence level the data is neutral as to the existence of anisotropies. Consequently, any detection of anisotropies, or lack thereof, must be at a lower confidence level.

In some circumstances statistical tests designed for the detection of signals in direct measurements, when applied to reconstructed images, will give reliable results. It has been shown that if the forward problem is linear, and has ideal signal and noise, and the reconstruction algorithm is linear with good resolution, such circumstances are achieved (Cover 2006).

## METHOD

The TOD for COBE consists of 3 pairs of channels. The frequency of each pair were 31.5, 53 and 90 GHz. Each channel pair had two polarisations labelled A and B. Channel 31B was not used in this reanalysis because of poor data quality. Bennett et

al. (1996), averaged together the sky maps of the A and B channel pairs after reconstruction to improve the SNR and displayed the results as a sky map for each frequency. In this analysis, the A and B channel sky maps will be presented separately to provide independent confirmation of the results.

For both the official reconstruction and this reanalysis the COBE TOD was fitted to a pixelized sky map,  $T_j$ , consisting of 6144 pixels. The fitting was accomplished for each channel using the maximum likelihood criterion.

The form of the COBE data used for the reanalysis were the “pixelized” differential data files from the official 4 year analysis and was downloaded from the Legacy Archive for Microwave Background Data Analysis (LAMBDA) web site maintained by the Goddard Space Flight Center. The pixelized data was calculated from the TOD by averaging together observations that had the same antenna directions in the pixelized sky. The data in the files included corrections for known systematic errors and subtraction of a nominal dipole.

The numerical optimization was implemented using the conjugate gradient algorithm (Press et al. 1992). Pixels further than a specified number of degrees from the galactic equator were constrained to zero by a simple method. First, the values for all pixels in all optimisations were set to zero. Second, for all pixels that were to be constrained to zero during an optimization, the corresponding gradient was forced to zero. This ensured that the required pixel values would remain unchanged at zero as desired. To correct for the monopole in each reconstructed sky map, the average value of all pixels more than  $30^\circ$  from the galactic equator was subtracted from every pixel in the respective sky map.

To double check the results of the reanalysis, the sky maps which had all pixels outside of  $24^\circ$  of the galactic equator forced to zero were used to generate simulated pixelized data. The simulated data was then reconstructed using the same reconstruction algorithm used in the official COBE analysis (which was maximum likelihood with all 6144 pixels unconstrained). The simulated data was generated without adding any instrumentation noise.

The smoothing and display of the sky maps closely follows the steps described in Bennett et al. (1996) including smoothing with a  $7^\circ$  Gaussian filter and the use of Mollweide projections. All calculations were performed on a PC with a 1200MHz Athlon CPU with 512MB of memory and written in Java. The time to calculate a single sky map for a single channel was between 5 and 10 minutes.

The official COBE analysis used the normalised  $\chi^2$  values in place of the actual  $\chi^2$  values. The normalised  $\chi^2$  values were calculated by dividing the actual  $\chi^2$  values by the number of TOD measurements,  $N$ . This convention was used in the reanalysis.

## RESULTS

Figure 1 shows how the normalised  $\chi^2$  values varies with an increasing number of constrained pixels for each of the 5 reconstructed channels. The increasing number of constrained pixels from  $90^\circ$  to  $24^\circ$  shows little change in the  $\chi^2$  values but below  $24^\circ$  they begin to show a distinct increase.

Table 1 shows comparisons between the sky maps produced by the official 4 year analysis of the COBE data and those reconstructed during the reanalysis from the pixelized data. The recalculated  $\chi^2$  values for the official sky maps and the sky maps reconstructed for the 5 channels with all pixels free to vary are within 3 parts per million of each other. The maximum absolute difference and the root-mean-square (RMS) of the difference between the sky maps do not exceed  $65.9\mu\text{k}$  and  $24.2\mu\text{k}$  respectively. The agreement between the  $\chi^2$  values of the official and reanalysis sky maps indicates the image reconstruction in the reanalysis is performing as expected.

Table 2 shows the precise value of the recalculated normalised  $\chi^2$  values for the official reconstruction from the official COBE analysis as well as the values from the reanalysis at  $90^\circ$ ,  $24^\circ$  and  $0^\circ$ . The percentage increase in the  $\chi^2$  values from the  $90^\circ$  to the  $24^\circ$  sky maps ranged between 0.21% and 0.24%.

Also in Table 2, the  $\chi^2$  values at  $0^\circ$  indicate how consistent the data from each channel is with a sky map with no signal. In both Fig. 1 and Table 2, all channels show a clear increase in the  $\chi^2$  values at  $0^\circ$  as compared to  $90^\circ$ . Channel 31A shows the highest increase of 3.3%, suggesting the poorest fit to no signal and thus the highest signal from the galactic band. Channels 53A and 53B show intermediate increases and channels 90A and 90B show the lowest at 0.61% and 0.74% respectively.

Figure 4 shows the sky maps reconstructed, with no pixels constrained to zero, from the simulated data from the  $24^\circ$  sky maps (shown in Fig. 3). No instrumentation noise has been added. Examination of the figure shows no signal outside the galactic band is visible.

## DISCUSSION

From the point of view of image reconstruction, the COBE sky map reconstruction problem is a particularly interesting one for several reasons. With the SNR of the reported detections of the anisotropies near unity, and with the galactic band radiating a much larger signal than the anisotropies, the COBE image reconstruction is particularly susceptible to false positive signal detection of anisotropies. Also, the maximum likelihood reconstruction algorithm used in the official COBE analysis does not take into account the variety of other sky maps which may also be consistent with the same TOD. In addition, there are many papers that describe the analysis of the COBE data in detail, thus facilitating any reanalysis. As an added bonus, within the next few years the Planck satellite will produce direct measurements of the same signals as the COBE sky maps, providing a "gold standard" against which to compare any reconstruction results.

### Averaging instrumentation noise

While this paper reanalyses the COBE data from the point of view of image reconstruction, the importance of the ideal noise assumption to the official COBE data analysis can be demonstrated in a simpler way. The instrumentation flight noise of the 5 channels reanalysed in this paper range from 23.13mK to 58.27mK for each 0.5s observation in the TOD (Bennett et al, 1996). The amplitude of the reported

anisotropies was roughly 44uK. Therefore, to reliably detect the anisotropies, the instrumentation noise must be reduced by at least a factor of 1000.

The official COBE analysis accomplished all its noise reduction by averaging. Explicit averaging was performed when the pixelized data was calculated from the TOD. Implicit averaging was performed as part of the sky map reconstruction from the pixelized data since the maximum likelihood reconstruction can be represented as a matrix multiplication. To reduce the instrumentation noise by a factor of 1000 would require the explicit averaging of 1,000,000 points assuming ideal noise. However, the implicit averaging taking place during the image reconstruction both adds and subtracts the weighted averages of the pixelized data. For a complete analysis, the official COBE analysis needed to show that the instrumentation noise behaved as ideal noise for more than 1,000,000 averages. The 0.7% uncertainty in the calibration of COBE TOD may have caused the instrumentation noise to deviate from the square-root-of-N rule characteristic of ideal noise at a values much less than 1,000,000 averages. Thus the sky maps reconstructed in the official COBE analysis may well show artefacts due to non ideal noise rather than anisotropies in the CMB.

### **Rejecting the null hypothesis**

To be able to reject the null hypothesis that there are no anisotropies outside the galactic band, we need a good estimate of the standard deviation of the  $\chi^2$  values over the 4 years of data acquisition. The noise of the TOD is reported in the official COBE analysis to be uncorrelated Gaussian (Kogut et al. 1996), and the official analysis assumed it to be ideal. As there were roughly 200,000,000 measurements for each channel, according to the probability theory presented in the Theory section of this paper, and the assumption of ideal noise, the standard deviation of the normalised  $\chi^2$  values would be roughly 0.000071. The normalised  $\chi^2$  values in the official COBE analysis actually varied over the channels from 0.93 to 1.18 as they do in this reanalysis. This discrepancy is discussed in Bennett et al. (1996) and is attributed to a change in the noise of the channels from pre-flight measurement to in-flight measurements. However, it is the change in the standard deviation of the noise over the 4 year mission, not the change at launch, that is important to the analysis.

The most likely source of variation in the  $\chi^2$  values over the 4 year mission is calibration errors in the TOD. As the amplitude of the noise is modulated by the gain, uncorrected calibration errors will have a direct impact on the stability of the instrumentation noise. The drift in gain over the 4 year mission is reported at less than 3% throughout the 4 year mission although post mission calibrations are reported to have reduced the drift to 0.7% over the whole 4 year mission. As the gain also applies to the noise, the stationarity of the noise is only known to about 0.7%. Therefore, a reasonable upper bound on the standard deviation of normalised  $\chi^2$  values is likely roughly 0.7% or 0.007.

Examination of Figure 1 in Kogut et al. (1996), initially appears to demonstrate the square-root-of-N rule is obeyed at up to nearly 10,000 averages, as would be expected from ideal noise. In particular, Kogut et al. noted that there was no indication of a noise floor. But careful examination of the curve shows a slight bulge between 1,000 and 10,000 samples that may indicate a slight deviation from the ideal noise

assumption. Small deviations from the ideal noise behaviour after this many averages is, very roughly, what might be expected from calibration drifts of under 0.7%.

Any deviation from the ideal noise assumption may be compounded by image reconstruction. The COBE reconstruction algorithm in the official analysis fitted the roughly 200,000 data points of the pixelized data to the 6144 pixels in the sky maps. Therefore, deviations in each pixelized datum by a small amount due to non ideal noise, may lead to inconsistencies in the fit and result in defuse patterns in the sky maps, possibly similar to anisotropies.

From Table 2, the differences between the  $\chi^2$  values of the official sky maps and the sky maps with all pixels outside of  $24^\circ$  of the galactic equator force to zero ranged between 0.20% and 0.27%. If the ideal noise standard deviation for  $\chi^2$  is used, the primary null hypothesis is rejected by  $141\sigma$  ( $0.0024/0.000071$ ) for channel 51B. This very high confidence level of detection is due to all the pixels outside of  $24^\circ$  of the galactic equator being included in the statistical test. However, as mentioned above, the better estimate for the standard deviation of the  $\chi^2$  is 0.7%, which is several times more than the  $\chi^2$  for 51B. Therefore the primary null hypothesis, that there are no anisotropies outside the galactic band, can not be rejected at any significant level for any of the channels.

Also from Table 2, the difference between the normalised  $\chi^2$  values of the official sky maps and the sky maps with all pixels force to zero, and thus zero signal everywhere, ranges between 3.3% and 0.61% of the normalised  $\chi^2$  values. Thus, assuming a standard deviation in the  $\chi^2$  values of 0.7%, the second null hypothesis, that there is no signal in each sky map, can be rejected for sky maps 31A, 53A and 53B. The rejection is questionable for 90A and 90B.

There is obviously signal in the galactic band for channels 90A and 90B. The failure to reject the second null hypothesis at any significant level may seem to suggest that the statistical test designed for image reconstruction has not performed properly. A more likely explanation is that we are seeing the consequences of the non ideal noise due to the uncertainty in the calibration.

Non ideal noise generated by calibration drift is likely to cause small errors in many observations rather than large errors in a few. For non ideal noise to generate signal similar to the galactic band would require large errors in a small fraction of observations which is not likely given the nature of the calibration corrections. The standard deviation of 0.7% is likely substantially overestimated for localised sources in the sky map, such as the galactic band, but should be a more reliable estimate for the defuse sources such as the anisotropies.

Figure 4 was included to see if the reported anisotropies were due to some artefact of the reconstruction similar to "truncation artefacts" in MRI. No anisotropies can be seen in Fig 4. While this does not completely eliminate the possibility that the reported anisotropies are not due to some sort of "truncation artefact", it provides no evidence to the contrary.

## **Independent verification of anisotropies**

A host of groups have reported detecting anisotropies in the CMB using ground based or airborne detectors. An extensive list of studies is included in Bennett et al. (2003). It may seem implausible to suggest that so many highly capable groups have all independently arrived at the same false positive detection of anisotropies. Nevertheless, such an occurrence is not unprecedented.

Matthews et al. (2004) reports an important example of many independent groups achieving the same false positive results due to a problem with the data analysis. They describe a case where at least 7 different ground-based studies reported the detection of p-mode frequencies in the photometry of the star Procyon. The confidence of the detection was so high that Procyon was considered one of the best candidates for asteroseismology.

However, the higher quality photometric data, returned by the MOST space-based telescope, showed the reported ground-based detections to be incorrect. Matthews et al. showed a possible cause of the repeated false positive detection of the p-mode frequencies could be traced to the algorithm used to reconstruct the frequency spectrum from ground based photometry. The reconstruction algorithm was based on the Fourier transform but was modified with the intent of handling gaps in the ground-based photometry due to the rotation of the earth. Matthews et al. showed these modifications could have inadvertently caused the false positive results. As we have much more experience using the Fourier transform in image reconstruction than we do with the image reconstruction algorithm used for COBE, the possibility of a false positive detection of anisotropies in the CMB due to image reconstruction needs to be given serious consideration.

The high correlation between the results of pairs of groups means that there must be information shared among the analyses. But this information does not have to be the signal from anisotropies as is assumed. For example, the choice of the same maximum likelihood fitting algorithm, with perhaps similar starting points for the optimization, may lead the reconstruction algorithms for different groups to converge on a similar type of sky map. The similarity would be in spite of the fact that there may be a large variety of sky maps consistent with the data for each group.

For example, the WMAP official analysis has reported results well correlated with those of COBE (Bennett et al. 2003). The WMAP mission design closely followed that of COBE with the major exceptions of larger antenna area and lower noise electronics. WMAP (1) used the reconstruction algorithm used by the COBE mission, (2) its reported calibration error after corrections was 0.5% which was similar to COBE's value and (3) used both explicit and implicit averaging to reduce the instrumentation noise when generating the sky map. As with COBE, the extensive use of averaging makes the sky maps susceptible to non ideal noise artefacts caused by uncertainty in the calibration. Thus, it would not be surprising if the WMAP data would also be unable to reject the null hypothesis that there were no anisotropies. Consequently, it would be worthwhile to repeat the reanalysis presented in this paper on WMAP TOD data. The outcome should be similar to that of the COBE TOD data.

## The Planck Satellite

The Planck mission is currently scheduled for launch in 2008. The current mission profile calls for 30 months of operations including two complete surveys of the full sky, each requiring between 12 and 14 months of observing time (Tauber 2004). The satellite will rotate at 1 revolution per minute. As the satellite rotates, the field of view will trace a circle of  $170^\circ$  on the sky. The circle will be displaced in small increments over each day so the total average displacement per day will be about  $1^\circ$ . Thus the whole sky will be scanned in about 6 months. The sky maps will be reconstructed from the many intersecting circles of data. The anisotropies reported by COBE should be detectable directly by Planck by averaging many repetitions of the same circle provided the measured signal behaves as ideal noise over the measurement time.

## CONCLUSIONS

The reported detection of CMB anisotropies by COBE might be explained as an artefact of non ideal noise in the official COBE analysis. The 0.7% calibration uncertainty in the COBE TOD may preclude the noise from obeying the square-root-of-N rule at the level of more than 1,000,000 averages which is implicitly assumed in the official COBE analysis. Therefore, the signal reported as anisotropies in the CMB in the official COBE analysis might be explained as image reconstruction artefacts of non ideal noise.

The Planck satellite should be able to provide a definitive answer as to the existence of 10 ppm anisotropies by direct measurement because of its single beam antenna and low noise performance. However, if the CMB anisotropies exist but are substantially less than 10 ppm, it is unclear how effective Planck will be in detecting them. If circumstances permit, some sort of prelaunch modification to Planck that would allow a wider beam size, which could be selected on orbit, in addition to the one currently planned, might be worth considering.

Nothing in this paper should be taken as a claim that anisotropies in the CMB at 10ppm or less do not exist. Rather, this paper questions the completeness of the official COBE analysis in ruling out all possible sources of structure in the sky maps outside the galactic band other than anisotropies. The conclusion of the reanalysis, that the amplitude of the systemic errors may exceed the reported anisotropies, depends on the proposed generalisation of rejecting the null hypothesis to sky maps and its correct application to the COBE data. Both these steps need careful review. Moreover, the noise characteristics of the COBE data, often assumed in the official analysis to be ideal, require additional detailed scrutiny.

## References

Barnes C., et al., 2003, "First year Wilkinson microwave anisotropy probe (WMAP) observations: Galactic signal contamination from sidelobe pickup," ApJS, 148, 51

Bennett C.L., et al. 1996, "4-Year COBE DMR Cosmic Microwave Background Observations: Maps and Basic Results," ApJ, 464, L1

ed. Bennett C.L., Leisawitz D, Jackson P.D., 1996B, "COBE-DMR Four-year project data sets (PDS), analyzed science data sets (ASDS), and galactic coordinate data sets explanatory supplements" COBE Ref Pub. No. 96-B (Greenbelt, MD; NASA/GSFC), available in electronic form from the NSSDC.

Bennett C.L., et al. 2003, "First year Wilkinson microwave anisotropy probe (WMAP) observations: preliminary maps and basic results," *ApJS*, 148, 1

Cover K.S., 2006, "A multiexponential reconstruction algorithm immune to false positive peak detection", *Rev. Sci. Instrum.*, In press (Currently available online at [rsi.aip.org](http://rsi.aip.org) in the July 2006 issue).

Frank L.R., Brossman J., Buxton R.B., Resnick D., 1997, "MR imaging truncation artifacts can create a false laminar appearance in cartilage", *American Journal of Roentgenology*, 168, 547

Istratov A.A, Vyvenko O. F., 1999, "Exponential analysis in physical phenomena", *Rev. Sci. Instr.* 70, 1233

Kogut A., Banday, A. J, Bennett C. L., Gorski, K. M., Hinshaw G., Jackson P. D., Keegstra, P., Lineweaver C., Smoot, G. F., Tenorio, L., Wright E. L., 1996, "Calibration and systematic error analysis for the COBE DMR 4 year sky maps," *ApJ*, 470, 653-673

Kogut A., Banday A.J., Bennett C. L., Gorski K. M., Hinshaw G., Smoot G. F., Wright E. L., 1996, "Microwave emissions at high Galactic latitudes in the four-year DMR sky maps," *ApJ*, 464, L5

Mather J.C., Boslough J, 1996, *The very first light: the true inside story of the scientific journey back to the dawn of the universe.* Basic Books, New York

Matthews J.M., Kusching R., Guenther D.B., Walker G.A., Moffat A.F.J., Rucinski S.M., Sasselov D., Weiss W.W., 2004, "No stellar p-mode oscillations in spaced-based photometry of Procyon," *Nature*, 430, 51

Press W.H., Teukolsky S.A., Vetterling W.T., Flannery B.P., 1992, *Numerical recipes in C.* Cambridge Univ. Press, Cambridge

Smoot G., 1992, "Structure in the COBE differential microwave radiometer: 1<sup>st</sup> year maps," *ApJ*, 396, L1

Smoot G., 1993, *Wrinkles in time: the imprint of creation.* Abacus, London

Spergel D.N. et al., 2003, "First year Wilkinson microwave anisotropy probe (WMAP) observations: determination of cosmological parameters," *ApJS*, 148, 175

Starkman G. D. and Schwarz D. J., 2005, "Is the universe out of tune?", *Scientific American*, 293, 48

Tauber J. A., 2004, "The Planck mission", *Advances in space research*, 34, 491

Tarantola A., 1987, Inverse Problem Theory, Elsevier, Amsterdam

Wood M.L., Henkelman R.M.,1985, "Truncation artifacts in magnetic resonance imaging", Magnetic resonance in medicine, 2, 517

## Figure Captions

**Figure 1.** Graph of the  $\chi^2$  values versus the number of degrees from the galactic equator beyond which the pixels in the sky maps were constrained to zero. As can be seen from the plots, there was virtually no change in the  $\chi^2$  values between  $90^\circ$  and  $24^\circ$ . The horizontal axis is labelled in units of degrees but is spaced by the percentage of pixels that are not constrained to zero.

**Figure 2.** Sky maps reconstructed as part of the reanalysis with none of the 6144 pixels constrained to zero and thus matching the official COBE reconstructions. The sky maps clearly show that the signal from the galactic band is many times larger than that of the apparent anisotropies.

**Figure 3.** Sky maps reconstructed, as part of the reanalysis, with pixels further than  $24^\circ$  from the galactic equator constrained to zero. These sky maps are, to within the corrected calibration errors from the official analysis, as consistent with the COBE TOD data as the official reconstructions.

**Figure 4.** Sky maps reconstructed from simulated data generated from the sky maps in Fig. 3 but with no instrumentation noise added. It is clear from the figure that the simulated data shows no significant anisotropies outside the galactic band.

**Tables****Table 1.** Comparison of the sky maps from the official 4 year analysis (Bennett et al 1996) and the sky maps reconstructed during the reanalysis. The maximum absolute difference and root-mean-square (RMS) difference between the sky maps are over all of the 6144 pixels.

Channel	Number of observations	Official Normalized $\chi^2$ (Bennett et al. 1996)	Reanalysis Normalized $\chi^2$ ( $b < 90^\circ$ )	Sky Maps Maximum Absolute Difference (mK)	Sky Maps RMS of Difference (mK)
31A	168,132,225	1.12118354	1.12118002	0.0659	0.0242
53A	218,557,665	1.05410507	1.05410233	0.0337	0.0131
53B	218,586,649	1.18123722	1.18123414	0.0337	0.0131
90A	218,398,620	0.93740230	0.93740007	0.0324	0.0078
90B	218,360,156	1.17461294	1.17460992	0.0260	0.0070

**Table 2.** The  $\chi^2$  values of the sky maps reconstructed during the reanalysis for no pixels constrained to zero ( $b < 90^\circ$ ), pixels outside  $24^\circ$  of the galactic plane constrained to zero ( $b < 24^\circ$ ), and all pixels in the sky maps constrained to zero ( $b = 0^\circ$ ). (The second column is reproduced from Table 1).

Channel	Reanalysis Normalized $\chi^2$ ( $b < 90^\circ$ )	Reanalysis Normalized $\chi^2$ ( $b < 24^\circ$ )	Reanalysis Normalized $\chi^2$ ( $b = 0^\circ$ )	Differences in Normalized $\chi^2$ ( $b = 24^\circ$ minus $b = 90^\circ$ )	Differences in Normalized $\chi^2$ ( $b = 0^\circ$ minus $b = 90^\circ$ )
31A	1.12118002	1.12359839	1.15818237	0.00241837	0.03700235
53A	1.05410233	1.05668081	1.07795510	0.00257848	0.02385277
53B	1.18123414	1.18397989	1.20146171	0.00274575	0.02022757
90A	0.93740007	0.93941973	0.94313518	0.00201966	0.00573511
90B	1.17460992	1.17721477	1.18330889	0.00260485	0.00869897

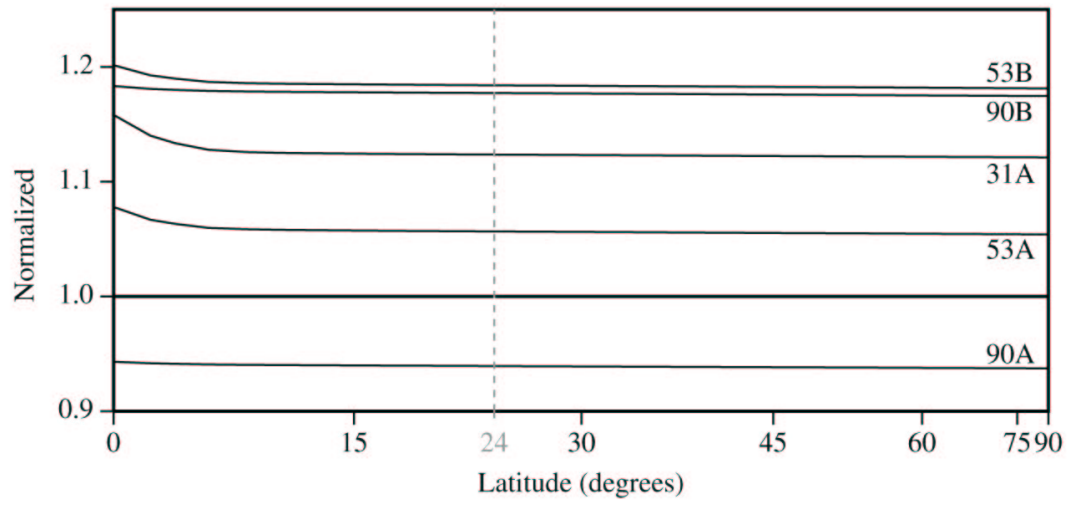


Figure 1

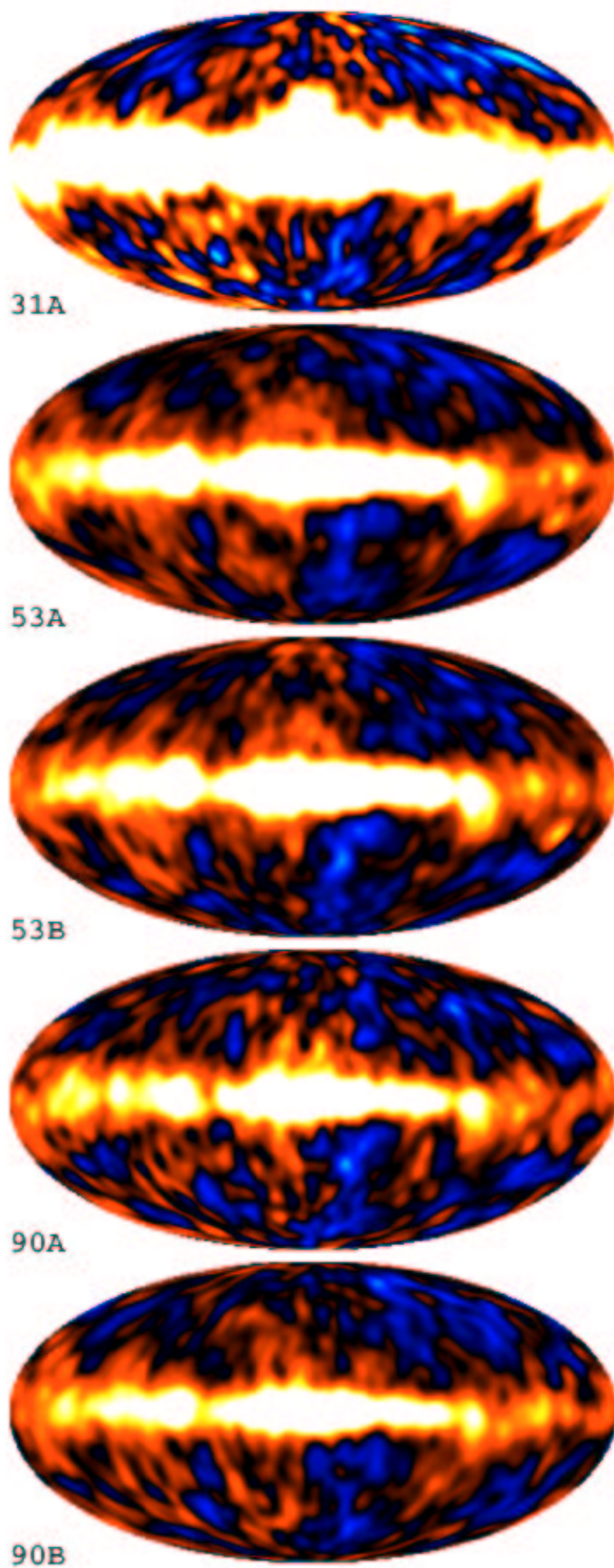


Figure 2

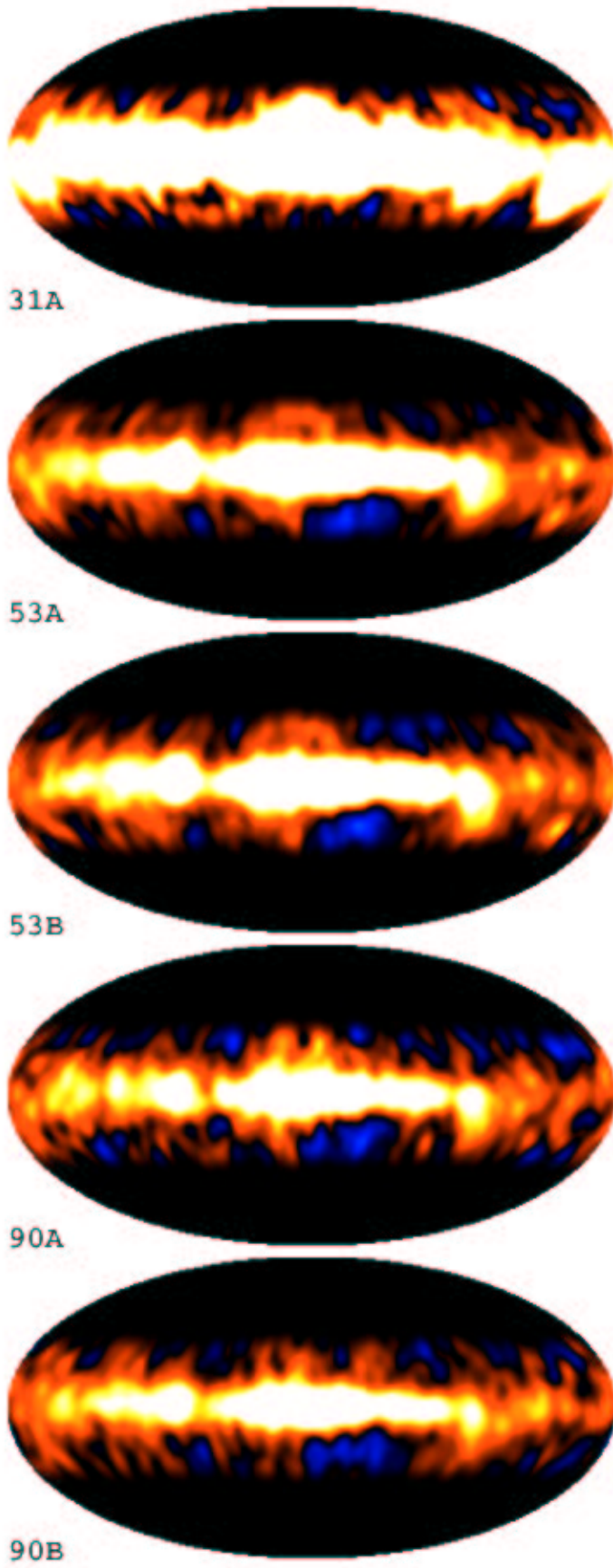


Figure 3

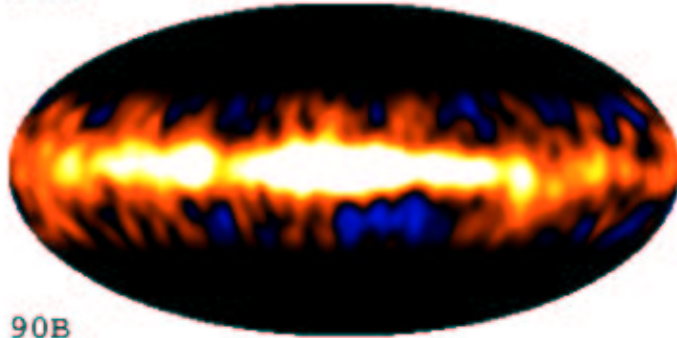
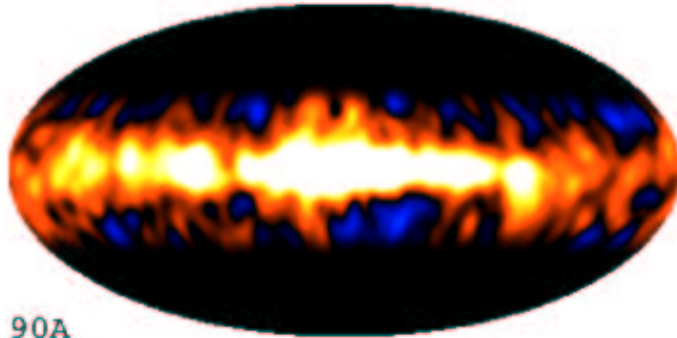
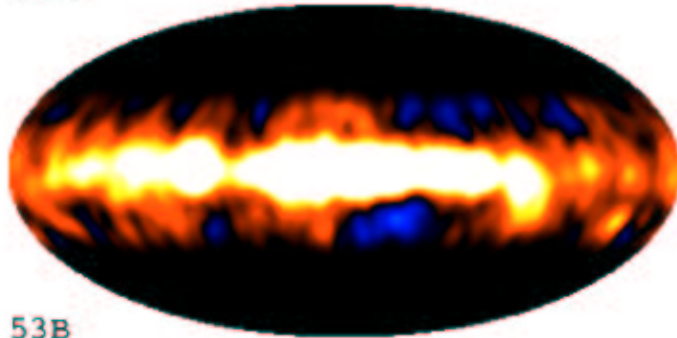
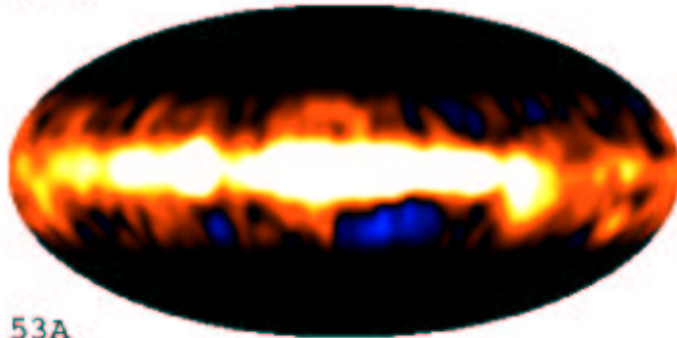
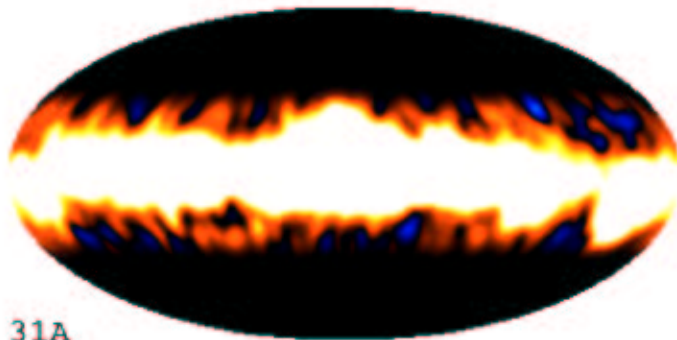


Figure 4